Chemistry & Biology
Article

Design, Synthesis, and Evaluation of In Vivo Potency and Selectivity of Epoxysuccinyl-Based Inhibitors of Papain-Family Cysteine Proteases

Amir Masoud Sadaghiani,[1] Steven H.L. Verhelst,[1] Vasilena Gocheva,[3] Kimberly Hill,[4] Eva Majerova,[4] Sherman Stinson,[5] Johanna A. Joyce,[3] and Matthew Bogyo[1,2,*]
[1] Department of Pathology
[2] Department of Microbiology and Immunology
Stanford School of Medicine, 300 Pasteur Drive, Stanford, CA 94305, USA
[3] Cancer Biology and Genetics Program, Memorial Sloan Kettering Cancer Center, 1275 York Avenue, New York, NY 10021, USA
[4] SAIC-Frederick
[5] Developmental Therapeutics Program
National Cancer Institute at Frederick, Frederick, MD 21702, USA
*Correspondence: mbogyo@stanford.edu
DOI 10.1016/j.chembiol.2007.03.010

SUMMARY

The papain-family cathepsins are cysteine proteases that are emerging as promising therapeutic targets for a number of human disease conditions ranging from osteoporosis to cancer. Relatively few selective inhibitors for this family exist, and the in vivo selectivity of most existing compounds is unclear. We present here the synthesis of focused libraries of epoxysuccinyl-based inhibitors and their screening in crude tissue extracts. We identified a number of potent inhibitors that display selectivity for endogenous cathepsin targets both in vitro and in vivo. Importantly, the selectivity patterns observed in crude extracts were generally retained in vivo, as assessed by active-site labeling of tissues from treated animals. Overall, this study identifies several important compound classes and highlights the use of activity-based probes to assess pharmacodynamic properties of small-molecule inhibitors in vivo.

INTRODUCTION

The papain family or clan CA is one of the largest and best-studied subfamilies of cysteine proteases. A number of enzymes in this family have been shown to be involved in physiological processes such as antigen presentation, bone remodeling, and transcriptional regulation as well as in important pathological processes such as rheumatoid arthritis, Alzheimer's disease, and cancer (for a review, see [1]). As a result, a significant effort has been made over the past 20 years to develop selective inhibitors of members of this family in order to gain a better understanding of the specific roles of these proteases in given disease states and as potential new therapeutics agents.

Surprisingly, only a few highly selective inhibitors for any of the cysteine cathepsins currently exist because development is hindered by the high degree of similarity in the primary S2 substrate-recognition pocket of these proteases. Perhaps the best example of a selective inhibitor is the compound CA-074, which contains the epoxysuccinyl reactive group found in the natural product E-64 [2, 3]. This compound was designed without the benefit of structural information, but it shows virtually exclusive reactivity with cathepsin B. The selectivity of CA-074 and related analogs was later determined to result from efficient hydrogen-bond interactions between a free carboxylic acid on the inhibitor and two histidine residues in the so-called occluding loop structure found only in cathepsin B [4, 5]. This compound and several related classes of compounds have been shown to retain a high degree of selectivity even when used in complex proteomes and intact cells [6–9].

Developing selective inhibitors of other papain-family proteases has been more difficult, and few examples of highly selective inhibitors have been reported [10]. One CA clan protease, cathepsin K, has recently received significant attention due to its role in bone remodeling [11]. In fact, several major pharmaceutical companies have active programs to target cathepsin K, and multiple compounds are currently in human clinical trials for osteoporosis [12]. Interestingly, at least one lead cathepsin K inhibitor in the clinic, while having selectivity profiles of 1000-fold or better over some cathepsin targets, is still a highly potent inhibitor of closely related cathepsin off-targets [13]. In addition, studies of pharmacodynamic properties of these lead compounds are often difficult to assess due to the lack of reagents that allow for direct analysis of specificity in a given tissue or cell population. In general, the process of drug discovery relies heavily on in vitro testing of lead compounds against purified enzyme targets to establish potency and selectivity properties. However, these properties may not be retained once the compounds are introduced into a whole organism, and actual specificity of

a given compound in a specific cellular location (i.e., in osteoclasts or tumor cells) is difficult to monitor. Several recent efforts with activity-based probes (ABPs) in intact cells and whole animals have demonstrated the value of these reagents for profiling inhibitor potency and selectivity within the context of a native cellular environment [14–17].

In this study, we describe the synthesis and screening of libraries of epoxysuccinyl-based inhibitors and subsequent analysis of several classes of novel lead compounds in vivo. We chose to use the epoxysuccinyl scaffold because general inhibitors in this class have been shown to have activity during multiple stages of tumorigenesis in mouse models of cancer, while displaying overall low toxicity [18], and have also been evaluated as therapeutics in human clinical trials for muscular dystrophy [19]. In addition, we believe that covalent inhibitors have the potential to be highly selective in vivo due to the permanent nature of the inhibition mechanism that allows specificity to be controlled by pharmacodynamic properties that dictate local concentrations of drug. Therefore, we chose to carry out initial screens in crude extracts to assess potency and selectivity properties and use this information to identify lead compounds. A series of optimized inhibitors was tested for standard pharmacokinetic properties and was also tested for overall in vivo specificity within given tissues by using activity-based protein profiling (ABPP). These studies show that it is possible to rapidly identify compounds with a range of selectivity profiles and potencies, and that these properties could be directly evaluated in specific cellular locations in vivo.

RESULTS

Design and Synthesis of Libraries of Epoxysuccinyl-Based Inhibitors

We initially set out to synthesize analogs of the general clan CA cysteine protease inhibitor E-64. A number of studies of this inhibitor scaffold have shown that specificity can be modulated by incorporation of structural elements on both sides of the symmetrical epoxysuccinyl functional group. Several classes of so-called ''double-headed'' epoxides that target CA clan proteases such as cathepsins B and L have been described [8, 9, 20, 21]. Furthermore, our group recently developed a solid-phase method that allows for direct synthesis of double-headed epoxides on resin, thereby allowing for rapid production of diverse classes of compounds [9]. We therefore initially designed a set of three sublibraries based on the general inhibitor JPM-OEt, which contains a tyramine-leucine core linked to the epoxysuccinate in the 2*S*,3*S* conformation (Scaffolds 1–3; Figure 1A). For these initial libraries, we used a small set of primary amines to introduce diversity into the region of the inhibitor shown to bind in the prime side binding pockets of the target cathepsins [5]. In addition to the tyrosine-leucine (2*S*,3*S*) epoxide library (Scaffold 3), we explored the contribution of the critical P2 residue by using a nonnatural p-methyl phenylalanine (Scaffold 1), shown previously to be an effective structural

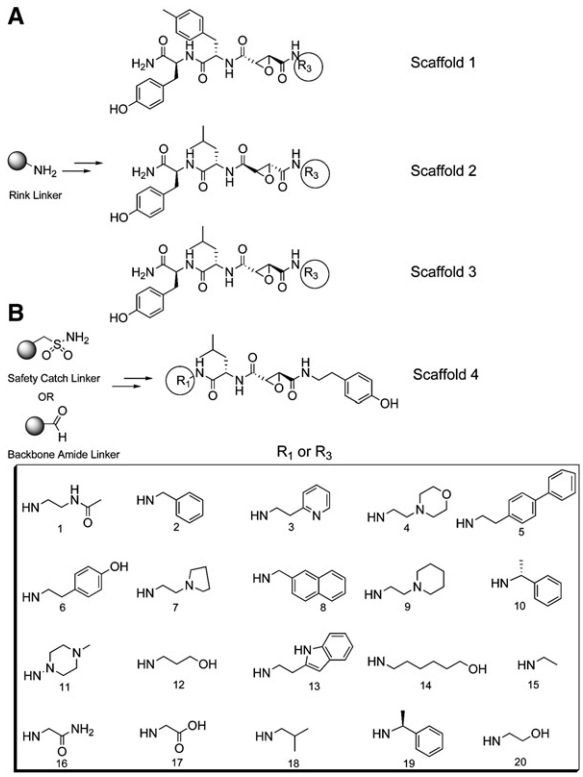

Figure 1. Solid-Phase Synthesis of Focused Epoxysuccinyl-Inhibitor Libraries

(A) Scaffolds 1, 2, and 3 were synthesized by using a previously reported method and were designed to incorporate diversity into the P2 and P1′ sites as well as to assess the importance of stereochemistry of the reactive epoxide group. These libraries contain diverse amines (structures shown at bottom) in the R3 position linked to scaffolds with two different P2 elements (leucine and p-methyl phenylalanine) and either *R*,*R* or *S*,*S* configurations of the epoxide.

(B) Scaffold 4 was synthesized by using two recently described synthesis methods. This library contains diverse amines in the R1 position with a fixed P1′ residue (tyramine). The structure and corresponding numbering of each amine used in the library synthesis are shown.

element in this position [22]. Finally, we created a scaffold in which the core tyrosine-leucine was retained but the stereochemisty of the epoxide was inverted to the (2*R*,3*R*) configuration (Scaffold 2). Previous work by our group and others has shown that this change in stereochemistry results in dramatic changes in the overall potency and specificity of inhibitors [22, 23]. For each scaffold, we synthesized a set of 17–20 individual compounds by using a subset of the diverse amines shown in Figure 1.

In addition, we evaluated the importance of the P3 element (R1 diversity site) by synthesizing a library of compounds in which the tyrosine residue of Scaffold 2 was replaced with our diverse amines and the R3 position was held constant as tyramine (Scaffold 4; Figure 1B). This library of 13 compounds was synthesized by using two solid-phase synthesis methods recently reported by our group [24] and was designed to both reduce the peptide

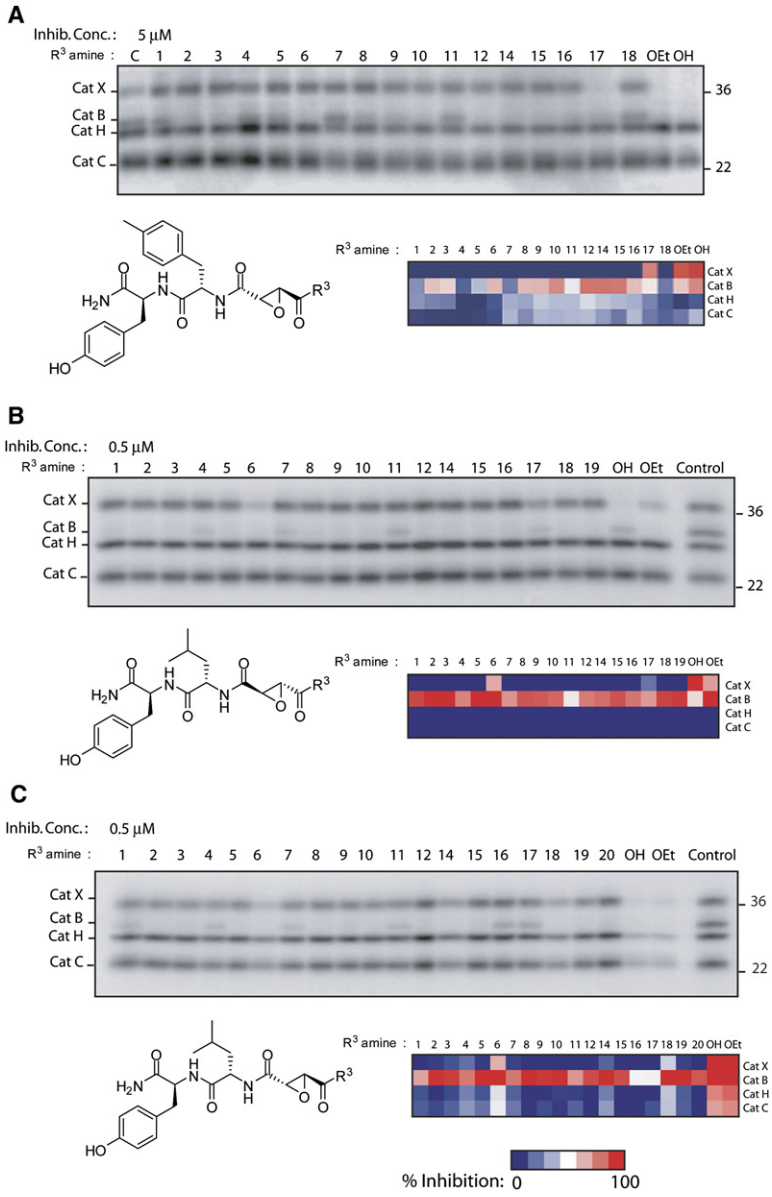

Figure 2. Screening of Libraries in Crude Rat Liver Proteomes

(A–C) Individual compounds from (A) Scaffold 1 library, (B) Scaffold 2 library, and (C) Scaffold 3 library were added to crude rat liver extracts (15 μg total protein) at the final concentration indicated. After a 30 min incubation, residual activity of several previously characterized cysteine cathepsin targets (identified at left of gel images) was assessed by labeling with the broad-spectrum papain-family protease probe ^{125}I-DCG-04. Samples were visualized by SDS-PAGE, followed by autoradiography. Values for percent competition relative to control DMSO-treated samples were determined for each compound and were plotted by using a colorimetric format in which the red signal is strong competition and the blue color is weak competition.

character of the inhibitors and to address the combined contribution of the P3 element to a compound with fixed P2 and P1′ elements.

Screening of Compound Libraries in Complex Proteomes

We and others have demonstrated the utility of screening small-molecule libraries in complex proteomes by using ABPs as readouts [22, 25, 26]. With this method, compounds are added to a proteome that contains multiple active targets, whose residual activity after compound incubation can be monitored by using a broad-spectrum active-site-directed probe. Thus, it is possible to directly monitor both the potency and selectivity of a given compound for multiple related targets without the need for significant quantities of recombinant enzymes and reporter substrates. In addition, results reflect activity against a native target protease that is present in a more physiologically relevant environment than a simple buffer system. We initially screened Scaffold 1–3 libraries by incubating compounds in total rat liver extracts at set inhibitor concentrations for 20 min. Samples were then labeled with the broad-spectrum ABP ^{125}I-DCG-04, and the residual activity of cathepsins was determined by SDS-PAGE, followed by autoradiography (Figure 2). Values for percent inhibition relative to the control DMSO-treated sample were determined by quantification of gel images and were used to plot specificity profiles for each compound by using a color format that facilitates visualization of the data.

The general probe ^{125}I-DCG-04, while capable of labeling all of the cysteine cathepsins when used with purified

recombinant enzymes [22], only labels cathepsins X, B, H, and C in the rat liver extracts. While it is likely that these are the primary active cathepsins in the extracts, it is not clear why the probe fails to label cathepsin L, which is expressed at high levels in the liver. This may be due to loss of activity of the enzyme upon disruption of the cellular compartments when making tissue extracts or may be due to the tight regulation of its activity in these tissues. We have previously shown that related compound ^{125}I-JPM-OEt efficiently labels active cathepsin L in intact cells, but not in extracts prepared from the same cell population [27]. Regardless of the potential shortcoming, we proceeded with library screening with a focus on the primary active cathepsins in the extracts.

Analysis of the initial screening data identified several interesting specificity trends. The most obvious of these trends was an overall high degree of selectivity of virtually all of the double-headed compounds for cathepsin B. Thus, regardless of the P2 element and the stereochemistry of the epoxide, addition of any amine (including simple ethyl amine) resulted in compounds with specificity for cathepsin B. Only amines 6, 14, 17, and 18 showed any crossreactivity with cathepsins X, H, and C (Figure 2). This was in stark contrast to the compounds containing a free acid or a simple ethyl ester on the epoxide, which showed broad reactivity toward all the active cathepsins. It was particularly surprising that the ethyl amide (amine 15) on Scaffold 1 was significantly more cathepsin B selective than the related compound in which this P1′ element was an ethyl ester. This result suggests that backbone hydrogen bonding in the S1′ region of cathepsin B may play an important role in dictating overall specificity and may also help to explain the high degree of selectivity of cathepsin B inhibitors that contain peptide elements in this region. Alternatively, the ethyl ester may be processed to the free acid when added to protein extracts, resulting in enhanced potency toward all cathepsin targets. We favor the former explanation, as we see significant differences in the potency of the free acid and ester forms of the general inhibitor JPM-OEt, suggesting that the ester must, to some extent, be retained in extracts.

A second important trend observed in the initial screening data was the overall change in specificity of compounds when the epoxide stereochemistry was inverted. In general, all compounds that contained the 2*R*,3*R* stereochemistry showed a complete lack of reactivity toward the two exopeptidases cathepsins H and C. In addition, an interesting change in specificity was observed for compounds that had a free carboxylic acid and ethyl ester in the P1′ site. These compounds went from being generally equipotent for cathepsins B and X and also relatively potent for cathepsins H and C in the context of the 2*S*,3*S* epoxide (Figure 2C) to showing cathepsin B selectivity for the ethyl ester and cathepsin X specificity for the free acid in the context of the 2*R*,3*R* epoxide (Figure 2B). Thus, these results confirm the importance of stereochemistry of the epoxide and provide additional structural elements that can be exploited to control the specificity of these compounds.

Synthesis and Pharmacokinetic Evaluation of a Series of Lead Compounds Designed Based on Initial Screening Data

We selected a series of compounds for evaluation in follow-on studies by choosing both R2 and R3 elements as well as epoxide stereochemistries that maximized either specificity for a given cathepsin target or overall reactivity toward all cathepsins (Table S1; see the Supplemental Data available with this article online). We chose several R2 elements, including the leucine and p-methyl phenylalanine used in the initial library scaffolds, but we also included two other nonnatural amino acids (norvaline and cyclohexylalanine) that had previously been shown to efficiently bind cathepsin targets [22]. These additional nonnatural amino acids were included to assess the effects of nonnatural P2 elements on the pharmacokinetic (PK) properties of the inhibitors. We selected amines 6, 12, and 17 for use in the R3 position and included a number of compounds with a free carboxylic acid in this position. The resulting set of 14 compounds (AMS1–AMS14) was synthesized and purified for use in in vivo PK studies. In addition, we included the previously characterized inhibitors JPM-OEt and JPM-acid that were shown to have anticancer activity in mouse models of pancreatic cancer ([18] and J.A.J. and M.B., unpublished data).

We carried out PK studies in normal mice by using intravenous (IV) or intraperitoneal (IP) injections or intragastric intubation (PO) of compounds at 50 mg/kg doses (Figure 3; Table S2). Serum levels of the compounds at various time points after injection were measured by using an LC/MS protocol (see Experimental Procedures). The resulting plots show that all of the compounds are detected in serum at high concentrations shortly after IV and IP injections, and that these concentrations drop rapidly over the next 30 min. While at least one compound was retained at concentrations over 1 μM at 120 min after IV injection, all seemed to show a similar trend of relatively rapid clearance. In addition, all compounds showed low or nondetectable levels after PO administration (see Table S2), suggesting that they were not readily absorbed by the oral route. This was not surprising since all of the compounds contained either a free carboxylic acid or a polar phenol group, thus potentially limiting their uptake. Past studies with related epoxysuccinyl analogs indicated that conversion of the free acid group on the epoxide scaffold to an ethyl ester resulted in a prodrug that showed improved oral availability and that was converted to the parent free acid once absorbed [28]. We therefore synthesized the ethyl ester versions of AMS1 and AMS7 and analyzed their uptake by PO administration compared to JPM-OEt (Figures 3B and 3C; Table S3). These results show that both compounds could be detected as their free acid products in serum after oral administration, and that the observed levels were similar to JPM-OEt. However, the overall concentrations of all of the compounds remained low, suggesting that additional optimization would be required to improve oral uptake.

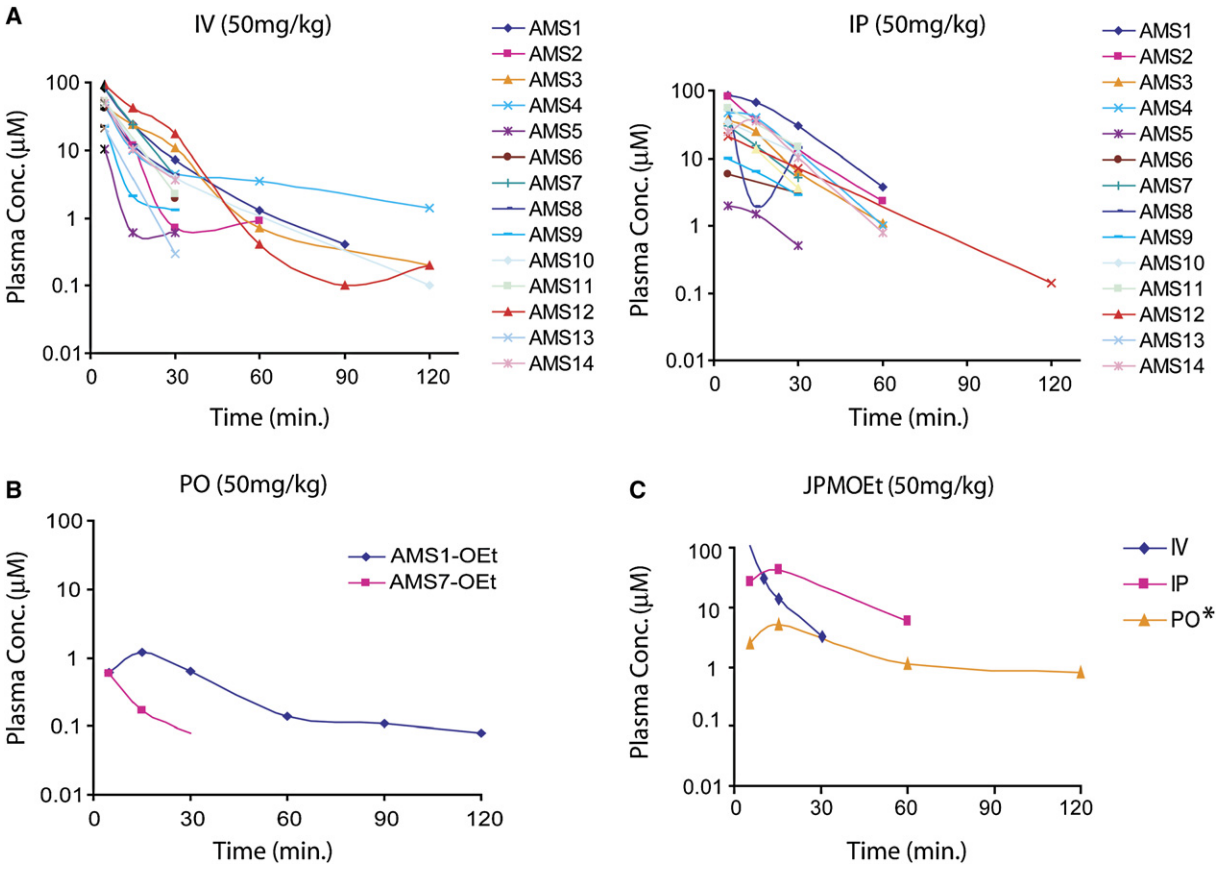

Figure 3. In Vivo Pharmacokinetic Properties of Compounds Derived from Initial Screening Data

(A–C) A total of 14 individual compounds (AMS1–AMS14; see Table S1 for structures) were selected based on predicted specificity or general reactivity for the cathepsins in rat liver extracts. Compounds were resynthesized, purified, and used to treat wild-type male nu/nu NCr mice at 50 mg/kg final concentrations. (A) Compounds were administered by intravenous (IV) and intraperitoneal (IP) injection, and serum levels of compounds were monitored at various times after injection by using a mass spectrometry-based readout. (B) Serum levels of ethyl ester versions of two of the original AMS compounds after oral administration (PO) at 50 mg/kg measured as in (A). Note: due to the rapid conversion of these esters to the free carboxylic acids in mouse serum, levels that were measured and shown here are for the corresponding free acids, and not for the parent ethyl ester pro-drugs. (C) Measurement of serum levels of the parent JPM-OEt after IV and IP injections as in (A). Oral availability of JPM-OEt determined as in (B).

Evaluation of In Vitro and In Vivo Potency and Selectivity of AMS1, AMS5, and AMS7

The overall potency and selectivity of each of the 14 AMS compounds were tested in rat liver extracts. Calculation of IC_{50} values from competition studies allowed us to prioritize compounds and select a set of three compounds with selectivity for cathepsin X, cathepsin B, or all cathepsins. The compound AMS1 was selected because it showed some degree of cathepsin X selectivity, while AMS5 was highly selective for cathepsin B. AMS7, a close relative to the parent compound JPM-565, was broadly reactive for all cathepsins in the lysates (Figure 4A). All three compounds were potent in the nanomolar range and were comparable in overall potency to the parent JPM-OEt (Figure 4B).

We next wanted to determine if the overall specificity profiles that we observed in crude liver extracts could be retained in vivo. For this study, we treated wild-type C57BL/6 mice at 13 weeks of age by IP injection with each of the compounds at 50 and 100 mg/kg daily for 5 days. At the end of the dosing, samples of tissues from liver and kidney were collected, and residual cathepsin activity was measured by in vitro labeling of tissue extracts with the radiolabeled probe ^{125}I-DCG-04 (Figure 4C). Like the parent compound JPM-OEt, all three analogs tested showed overall low acute toxicity, as measured by the normal appearance of the animals and their general good health throughout the 5 day course of treatment. Analysis of residual cathepsin activity in the tissues of treated mice indicated that all three compounds were able to gain at least partial access to pools of cathepsins in the liver and kidney. Not surprisingly, uptake in the liver was more efficient than in the kidneys, as measured by more complete inhibition in liver tissues for all compounds tested. More importantly, the pattern of specificity for each compound closely matched the patterns observed in vitro, with AMS1 showing the most effective inhibition of cathepsin X, AMS5 showing more selective inhibition

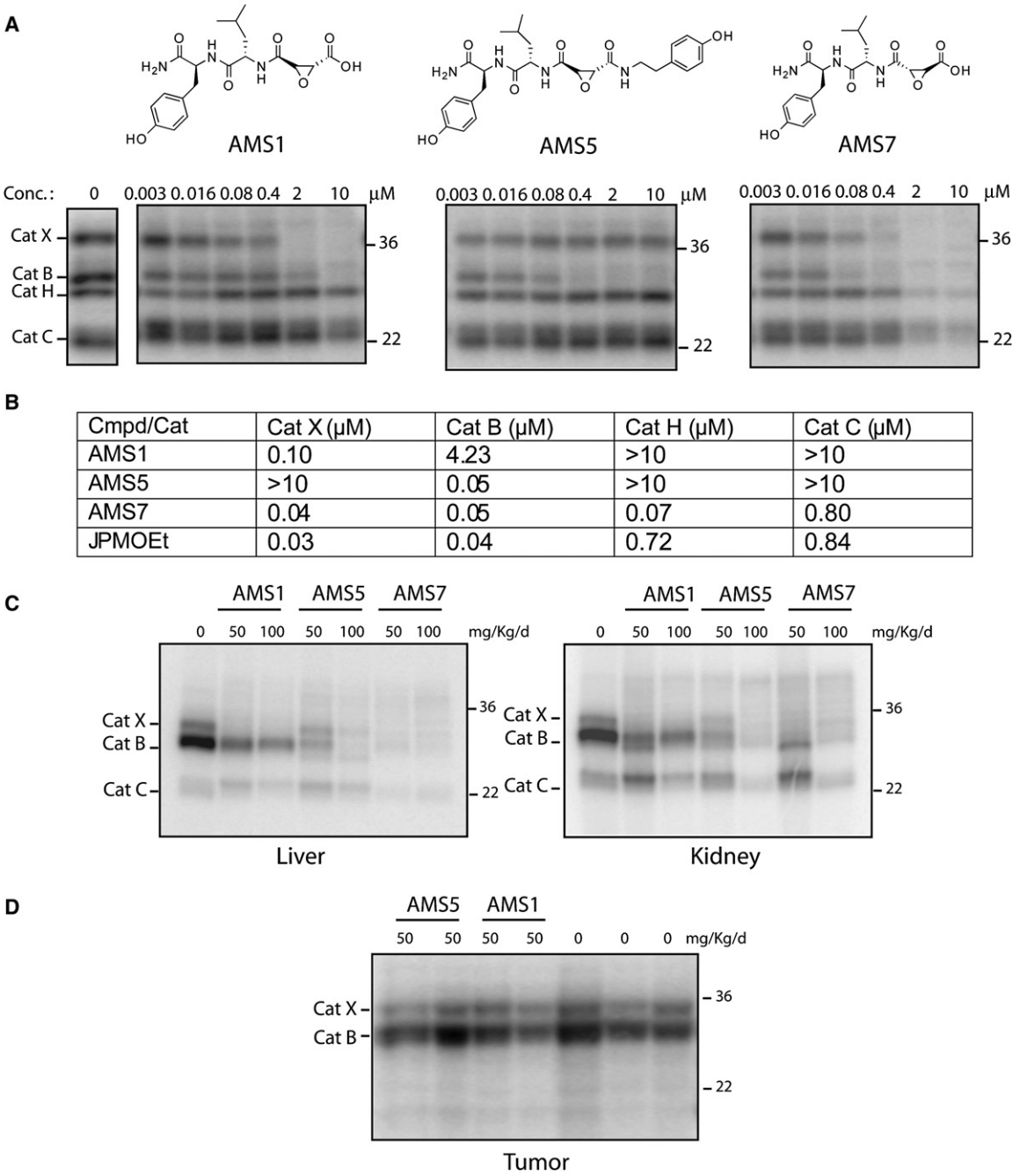

Cmpd/Cat	Cat X (μM)	Cat B (μM)	Cat H (μM)	Cat C (μM)
AMS1	0.10	4.23	>10	>10
AMS5	>10	0.05	>10	>10
AMS7	0.04	0.05	0.07	0.80
JPMOEt	0.03	0.04	0.72	0.84

Figure 4. In Vitro and In Vivo Specificities of Selected AMS Compounds from Scaffolds 1, 2, and 3

(A) Dose-response profiles of AMS1 (Cat B- and X-selective), AMS5 (Cat B-selective), and AMS7 (general) in crude rat liver lysates assessed by competition for labeling with ^{125}I-DCG-04.

(B) Quantification of IC_{50} values for AMS1, AMS5, and AMS7 against cathepsins X, B, H, and C based on the dose-response profiles in (A).

(C) In vivo selectivity of AMS1, AMS5, and AMS7 assessed by treatment of normal mice at doses of 50 and 100 mg/kg daily for 5 days. Tissues from control (DMSO vehicle-treated) and inhibitor-treated mice were collected, homogenized, and labeled with the general probe ^{125}I-DCG-04 to reveal residual activity.

(D) In vivo activity of AMS1 and AMS5 in RIP1-Tag2 tumors after IP treatment of tumor-bearing mice at 50 mg/kg daily for 5 days. Residual cathepsin activity in tissues was measured as in (C). Samples from two mice from each compound at the same dose are shown.

of cathepsin B, and AMS7 showing general inhibition of all of the cathepsin targets in both tissues. This result was particularly interesting because it suggests that even after prolonged treatment regimens, the fast clearance of the compounds and the irreversible mechanism of inhibition may help them to retain target selectivity.

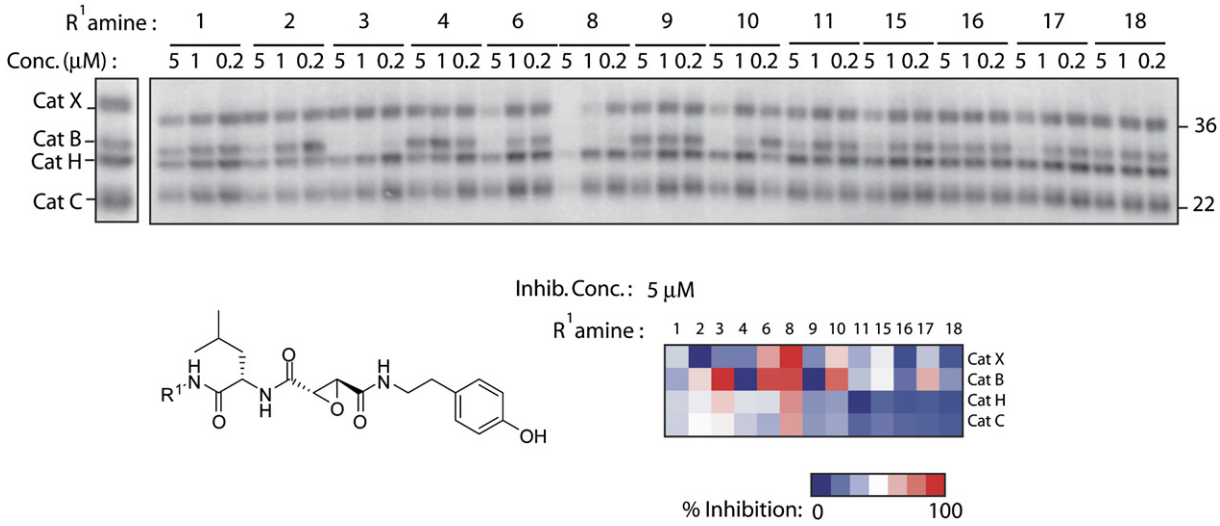

Figure 5. Screening of the Scaffold 4 Library and Identification of Optimal R1 Elements

Individual compounds from the Scaffold 4 library containing 13 diverse amines were added to crude rat liver extracts for 30 min at a range of concentrations as indicated. Residual activity of cysteine cathepsins was assayed by labeling of the extracts with ^{125}I-DCG-04, followed by analysis by SDS-PAGE. As in Figure 2, percent competition values were converted to color values and plotted for the series. Note that amine 3 and amine 8 were the only species that showed significant activity.

In addition, we tested the ability of AMS1 and AMS5 to block activity of cathepsin targets in tumor tissues from the RIP1-Tag2 transgenic mice used in earlier studies with the parent JPM-OEt [18]. AMS7 was not tested because of its close similarity in structure to JPM-OEt, which has been extensively tested in this model. We carried out IP injections of tumor-bearing mice at 13 weeks of age for 5 days at the dose of 50 mg/kg as previously described for the normal controls. Samples of dissected tumors from two mice treated with each compound were analyzed by active-site labeling with ^{125}I-DCG-04 (Figure 4D). These results indicated that, while there was some degree of variability in both the samples and the controls, both compounds failed to significantly reduce the activity of two primary cathepsin activities (cathepsins B and X). This is likely due to reduced accumulation and poor uptake for these free acid-containing compounds in tumor tissues.

Evaluation of Scaffold 3 Inhibitors with Variable P3 Elements and Reduced Peptide Character

While we were able to obtain some selectivity for specific cathepsin targets and this overall specificity was retained in vivo, the uptake and cell permeability of this first generation of lead compounds into tumor tissues was low. We therefore set out to analyze the Scaffold 4 library and determine if we could increase potency as well as cellular uptake by reducing the number of amide bonds in the compounds. The primary advantage of this scaffold is that it allows us to replace the amide bond used for resin attachment with simple amines.

We designed the Scaffold 4 library to contain a tyramine element in the P1′ position since we found that this residue strongly favored binding to cathepsin B (i.e., AMS5). Screening of the library of compounds in rat liver extracts at a range of concentrations identified several amines that could be used to generate cathepsin B-selective compounds (Figure 5). Interestingly, the compound made with amine 6 was nearly identical in structure to AMS5, but it was a relatively weak, though selective, inhibitor of cathepsin B. Thus, we lost significant potency by replacing the tyrosine with tyramine, potentially as a result of loss of hydrogen bonding of the backbone amide in the active site. However, two amines showed interesting patterns of potency and selectivity. Amine 3, which contained a pyridine ring, showed potent and selective inhibition of cathepsin B, while amine 8, which contains a bulky naphthyl group, produced a compound with broad reactivity for all of the cathepsin targets. These two amines were used to make a class of follow-on lead compounds that also made use of the information from our earlier screening efforts with Scaffolds 1–3.

Synthesis and In Vitro and In Vivo Evaluation of an Advanced Lead Series

As a final step in our medicinal chemistry efforts, we designed a series of four compounds that contained optimal pharmacophores at each of the R1, R2, and R3 sites, which made use of the *R*,*R* and *S*,*S* stereochemistry of the epoxide (Figure 6A). We designed the compound AMS17 to be cathepsin B selective by using the pyridyl ethyl amine (amine 3) in the P3 position, leucine in the P2 position, and tyramine in the P1′ position. AMS28 was designed to target all cathepsins and made use of the naphthalenemethyl amine in the P3 position to enhance potency. In addition, the ethyl ester was chosen for the P1′ site to prevent unwanted specificity toward cathepsin B. We also incorporated the naphthalenemethyl

A

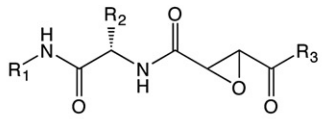

Inhibitor	R^1	R^2	R^3	Conformation	Target
AMS17	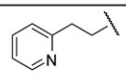		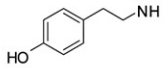	S,S	Cat B
AMS28	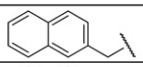		OEt	S,S	General
AMS30	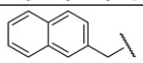		OEt	R,R	Cat B&X
AMS36	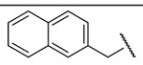	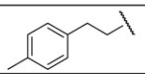	OEt	S,S	Cat X

B

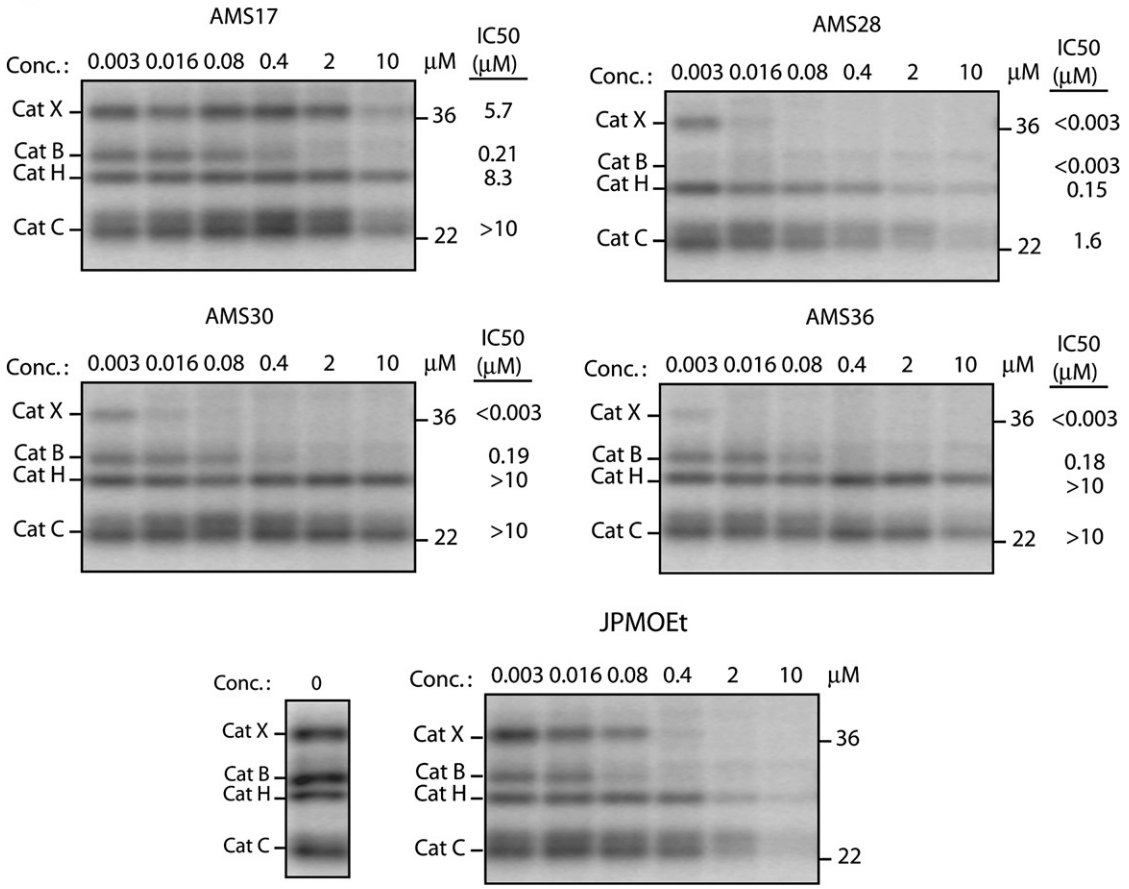

Figure 6. In Vitro Specificity Profiles of Optimized Lead Compounds

(A) A series of four compounds (AMS17, AMS28, AMS30, and AMS36) that were optimized based on all screening data were selected for further analysis of potency and selectivity (see chart at top).

(B) In vitro dose response was assessed by treatment of rat liver extracts at a range of concentrations, followed by labeling with ^{125}I-DCG-04. Samples were analyzed by SDS-PAGE, followed by autoradiography. Data for the parent compound JPM-OEt are included for comparison. IC_{50} values for each compound against each of the four cathepsins are shown to the right of the gel images. The control untreated sample used to calculate the IC_{50} values is shown at the bottom of the figure.

amine into the P3 position of AMS30 and used the *R*,*R* stereochemistry of the epoxide to direct specificity toward only cathepsins B and X. Finally, we used the naphthalenemethyl amine P3 in AMS36 and incorporated the non-natural p-methyl phenylalanine in the P2 position to increase the potency toward cathepsin X.

Analysis of the in vitro potency and selectivity of AMS17, AMS28, AMS30, and AMS36 in rat liver extracts indicated that all of the predicted specificity patterns were obtained (Figure 6B). In particular, AMS17 was highly specific for cathepsin B, while AMS36 had some degree of specificity for cathepsin X. In addition, AMS28 was an extremely potent and broad-spectrum inhibitor that showed enhanced potency compared to the parent JPM-OEt. Finally, AMS30 was extremely potent and selective for both cathepsin B and cathepsin X and showed no crossreactivity with cathepsins H and C even at high concentrations. Thus, we could achieve enhanced potency and selectivity for specific cathepsin targets by using optimal specificity elements from all three variable positions on the inhibitor scaffold.

Finally, we tested our advanced leads in vivo to determine if our observed in vitro specificity profiles were retained in various tissues of the RIP1-Tag2 transgenic mice. As described for our initial lead compounds, each of the advanced leads (AMS17, AMS28, AMS30, and AMS36) was IP injected at final concentrations of 50 and 100 mg/kg daily for 5 days. Tissues from liver, kidney, and tumors were harvested and analyzed by active-site labeling with ^{125}I-DCG-04 (Figure 7). Unfortunately, the solubility of AMS36 proved problematic and required the use of high concentrations of DMSO in the formulation of the drug. Therefore, we were only able to administer the drug for a single day due to toxicity to the animals. In addition, AMS28 showed significant toxicity at both doses, and, as a result, mice treated at the higher dose (100 mg/kg/day) had to be sacrificed. These issues with toxicity and formulation are most likely due to the increased hydrophobicity (formulation) and increased cell permeability and potency (toxicity) of the advanced lead series that contain the P3 amines. However, further evaluation of these issues, including lowering the dosage, will be required.

Regardless of the toxicity and formulation issues, we were able to harvest tissues from all of the mice and analyze the potency and selectivity of the compounds. As expected, AMS28 completely blocked the activity of all cathepsins in all tissues, including the tumors. In addition, it showed significantly enhanced potency and cell permeability relative to the related compound, AMS7. The cathepsin X-specific inhibitor AMS36 showed broad-spectrum inhibition in the liver with some degree of cathepsin X selectivity in the kidney at the lower dose of 50 mg/kg. Interestingly, this compound showed cathepsin X selectivity in tumor tissues at both doses tested. AMS30, on the other hand, showed highly selective cathepsin X and cathepsin B inhibition in all tissues, likely due to the fact that it contains the *R*,*R* epoxide, which precludes binding to cathepsins H and C. Surprisingly, we observed an enhanced labeling of cathepsin H and C in liver and kidney tissues relative to the control samples suggesting a potential upregulation or loss of turnover of these cathepsins as a result of inhibition of cathepsins B and X. Similar findings have been reported for other cathepsin targets in other in vivo models [29]. Finally, the cathepsin B-specific compound AMS17, like AMS36, seemed to accumulate in liver and kidney and therefore blocked the activity of all cathepsins in those tissues at the higher doses of drug, but retained some degree of selectivity for cathepsin B in tumor tissues. Overall, these results suggest that this class of advanced leads shows enhanced potency and cell penetration, leading to loss of specificity in tissues such as liver and kidney, where the compound accumulated. However, these compounds were able to selectively inhibit target cathepsins within less accessible tissue such as the RIP1-Tag2 tumors.

Since we were unable to determine the selectivity of our compounds toward several cysteine cathepsins (i.e., cathepsins K, S, V, F) as a result of their low or nonexistent expression levels in the tissues used in this study, we decided to test all of the leads against recombinant human cathepsins V and L (Figure S1). As expected, at the relatively high concentration of 1 μM the broad-spectrum inhibitors (AMS7, AMS28) were effective inhibitors of both enzymes. Similarly, the compounds that showed cathepsin B and cathepsin X selectivity in vivo (AMS30, AMS36) were also somewhat potent inhibitors of cathepsins V and L. In addition, AMS17, which showed cathepsin B selectivity in rat liver extracts, was quite potent against both cathepsins V and L, while AMS1 and AMS5 were relatively ineffective inhibitors of these targets. Overall, these results suggest that our optimal compounds may show some crossreactivity with other cysteine cathepsin targets; however, this crossreactivity will only be an issue in tissues in which these targets are expressed and in which the compounds accumulate.

DISCUSSION

The papain fold cysteine proteases are a relatively small family of enzymes (11 total in the human genome) that play a surprisingly diverse set of roles in both normal and disease processes. The critical role for proteases such as cathepsin K in bone remodeling has made it a hotly pursued drug target, with several advanced programs currently entering or already in clinical trials [12]. Thus, new methods to rapidly profile the in vivo specificity of inhibitors of this family of enzymes are of great value. Some of the most critical parameters that need to be determined in order to make sense of preclinical and clinical data are (1) did the drug get access to the target enzyme? and (2) does the compound retain its specificity in the relevant disease tissue or cell population? Often these parameters are difficult to determine, leading, in some cases, to early termination of discovery programs or late-stage failures of drugs due to undesired off-target activities. We describe here the use of small-molecule screens in relevant tissue extracts to identify lead compounds that can then be evaluated for in vivo potency and selectivity within specific tissues. The results from our synthesis, screening, and in vivo testing suggest that specificity profiles observed for covalent inhibitors with rapid clearance seem to be retained in tissues after systemic administration. Furthermore, the absolute selectivity of a given compound seems

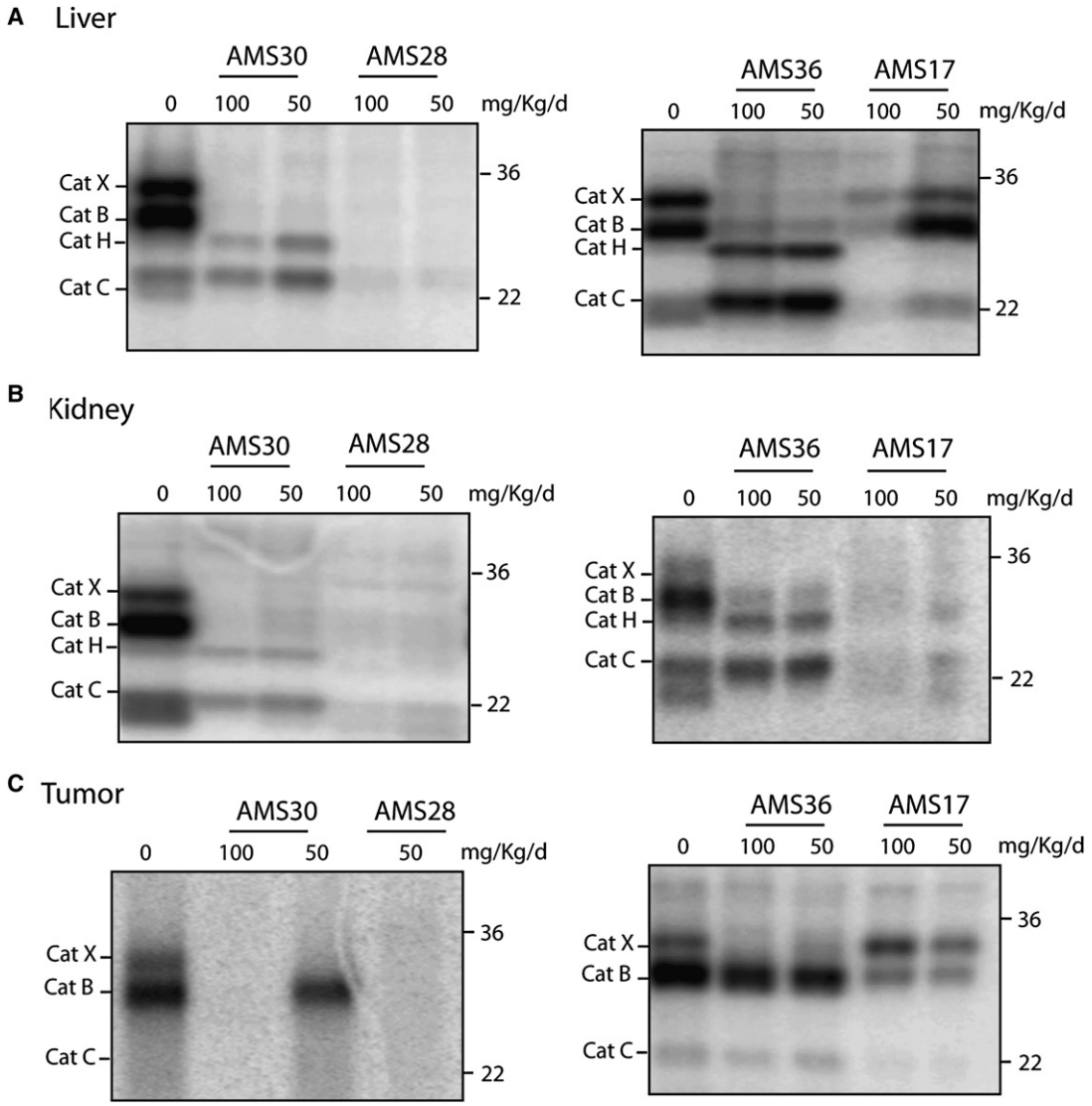

Figure 7. In Vivo Potency and Selectivity of Final Lead Compounds

(A–C) In vivo selectivity of AMS17, AMS28, AMS30, and AMS36 was assessed by treatment of normal mice at doses of 50 and 100 mg/kg daily for 2 days. (A) Liver and (B) kidney tissues from control (DMSO vehicle-treated) and inhibitor-treated mice were collected, homogenized, and labeled with the general probe ^{125}I-DCG-04. Samples were analyzed by SDS-PAGE, followed by autoradiography. AMS36 was injected in high-DMSO concentrations and could only be administered for 1 day. (C) RIP1-Tag2 mice at 13 weeks of age were injected with AMS28, AMS30, and AMS36 at doses of 50 and 100 mg/kg as in (A) and (B). Tumor tissues from control and treated animals were removed and analyzed for residual cathepsin activity as in (A) and (B). AMS28 showed significant toxicity in these animals at the higher dose of 100 mg/kg, and the study had to be discontinued at this dose. Thus, only data from the 50 mg/kg dose are shown.

to be controlled by its ability to access specific cellular locations. Thus, these data highlight the need to use highly sensitive methods such as activity-based profiling to determine key in vivo specificity parameters in order to evaluate and select new drug leads for advancement into human clinical trials.

Motivated by our initial, promising results for the parent compound JPM-OEt in the RIP1-Tag2 mouse model of pancreatic cancer [18], we set out to identify a series of lead compounds with diverse specificity and biodistribution patterns for further evaluation in this cancer model. We have chosen to use a competition-based screen with the ABP ^{125}I-DCG-04 since it allows us to screen relatively small libraries of compounds in a complex proteome that contains multiple active cathepsin targets. Thus, by using this method we do not need to obtain significant quantities of purified recombinant cathepsins, and we select for compounds that perform well in the context of the complex cellular environment. In the past, we have used this method to screen libraries against targets for which no recombinant source of enzyme was available [22, 25]. In this study, we demonstrate that an additional

benefit of carrying out initial screens with this method is the overall high degree of correlation of specificities and potencies with results obtained in vivo. Thus, we believe that this method has significant value for use in early drug development when a focused lead series is identified and small follow-on libraries of compounds are generated through medicinal chemistry efforts. In addition, while our study makes use of covalent inhibitors, the use of this screening method has been reported for classes of reversible inhibitors as well [26].

We found it somewhat surprising that our covalent inhibitors were generally able to retain their selectivity in vivo since we assumed that over time they would productively inhibit all targets as a result of the irreversible nature of their inhibition mechanism. In general, we observed a pattern in which selectivity was controlled by the access of the compound to the target proteases. In the liver, compounds accumulated, and specificity was only retained for compounds that had poor overall cellular uptake, while compounds that showed significant cellular permeability lost all selectivity. The kidney, while also involved in the filtering of small molecules from the blood, in general accumulated these molecules to a lesser extent than the liver. As a result, many of the non-cell-permeable compounds were not able to block intracellular pools of cathepsins. The RIP1-Tag2 tumors in the pancreas represent the relevant disease tissue in which inhibition of target cathepsins is desired. We observed potent and selective activity of compounds in tumor tissues, most likely due to the reduced delivery of the compounds to these tissues. Thus, compounds that are able to selectively and efficiently knock down cathepsin activities in tumor tissues are most likely going to induce broad-spectrum inhibition of cathepsin targets in other major organs such as the liver.

It should be pointed out that the relevant pool of active cathepsins that may be critical for disease pathogenesis may differ for each disease state. In the case of the RIP1-Tag2 model, we have observed therapeutic effects with compounds that do not readily penetrate cells (J.A.J. and M.B., unpublished data), suggesting that extracellular cathepsins secreted by both tumor cells and cells of the local microenvironment may be the critical pool to target with small-molecule inhibitors. This extracellular pool likely represents a small fraction of the total pool of active cathepsins inside the cell and thus could be effectively blocked without showing any significant drop in the total amount of active cathepsins, as measured in tissues extracts by using an ABP. In addition, compounds that show short half-lives in serum, but that permanently inhibit their targets and have reduced access to intracellular targets, may provide maximal efficacy with minimal toxicity. For this reason, we plan to use several of the compounds reported in this study for extended drug trials in the RIP1-Tag2 mice in the near future. These studies will help to correlate efficacy against the disease with inhibition and specificity of the lead compounds. In addition, these studies will help to further define the correlation of cell permeability and target inhibition with observed toxicity.

SIGNIFICANCE

The processes of compound screening, lead optimization, and preclinical evaluation are time consuming and expensive parts of the drug discovery process. In most cases, compound libraries are screened in vitro against a purified target that has been validated by basic biological and pharmacological studies. Only after extensive in vitro screening is a lead series identified for advancement into optimization and eventual testing in vivo. Often compounds are advanced into preclinical testing in animal models and even into early human clinical trials with only a limited understanding of in vivo potency and target selectivity in specific tissues and cell populations. We report here the synthesis and screening of several small and focused libraries of epoxysuccinyl-based inhibitors in the CA family of cysteine proteases. These libraries were used to identify compounds that showed interesting potency and selectivity in crude tissue extracts that could then be rapidly evaluated in vivo by using an activity-based profiling method. This in vivo profiling method allowed us to monitor the extent of target modification in different tissues and provided a direct readout of the overall specificity of compounds in a specific tissue of interest. Our results suggest that this class of compounds shows overall rapid clearance in serum, resulting in specificity profiles that are controlled by access of compounds to a given tissue or cell population. While we have by no means developed compounds with absolute specificity for any single cathepsin target, these results have highlighted a number of important specificity determinants on the epoxysuccinyl scaffold. In addition, this work has identified several valuable lead compounds that can be used to assess the importance of potency, cell permeability, and target selectivity of therapeutic agents designed to target clan CA proteases.

EXPERIMENTAL PROCEDURES

General Methods

Unless otherwise noted, all resins and reagents were purchased from commercial suppliers and used without further purification. All solvents used were of HPLC grade. Reverse-phase HPLC was conducted on a C_{18} column by using an ÄKTA explorer 100 (Amersham Pharmacia Biotech). LCMS data were acquired using an API 150EX LC/MS system (Applied Biosystems).

General Solid-Phase Synthesis Method

Solid-phase synthesis of all compounds was carried out using methods recently reported by our group [9, 24]. Solid-phase reactions were conducted in polypropylene cartridges (Applied Separations, Allentown, PA) with 3-Way Nylon Stopcocks (BioRad Laboratories, Hercules, CA). The cartridges were connected to a 20 port vacuum manifold (Waters, Milford, MA) that was used to drain solvent and reagents from the cartridge. The resin was gently shaken on a rotating shaker during solid-phase reactions.

Inhibitor Evaluation

Rat liver homogenate (20 μl; 1 mg/ml) in reaction buffer (50 mM sodium acetate, 2 mM DTT, 5 mM $MgCl_2$ [pH 5.5]) was incubated for 30 min

with inhibitors at indicated concentrations. Subsequently, ^{125}I-DCG-04 (10^6 cpm in 1 μl) was added, and the samples were incubated for 1 hr. Samples were quenched by the addition of 4× SD sample buffer, and samples were boiled for 5 min. Proteins were resolved by SDS-PAGE, and the labeled cathepsin activities were visualized by autoradiography by using a Typhoon 9410 imager (Amersham Biosciences). Densitometry was performed by using NIH-Image software. Numerical values for percent inhibitions were determined and converted to heat maps by using the programs Tree View and Cluster, written by Mike Eisen (http://rana.lbl.gov/EisenSoftware.htm), as reported previously [22]. Established numerical values for percent inhibitions were applied by using GraphPad Prism 4 software to determine the observed IC_{50} values, as given in Figure 4B.

In Vivo Inhibitor Treatment

Each of the AMS inhibitors was dissolved in a solution of DMSO/H_2O. Control C57BL/6 mice and RIP1-Tag2 mice [30] at 13 weeks of age were treated twice daily with an IP injection of each inhibitor or vehicle control (DMSO/H_2O) at doses of 50 mg/kg/day or 100 mg/kg/day for 2–7 days. The final inhibitor dose was administered 1 hr prior to sacrifice. Mice were then anesthetized with an IP injection of 2.5% avertin and were heart perfused with PBS. All organs were collected immediately and frozen in liquid nitrogen. Organs were weighed and dounced in lysis buffer (50 mM acetate [pH 5.5], 5 mM $MgCl_2$, 250 mM sucrose, and 2 mM DTT) and centrifuged at 14,000 × g for 20 min at 4°C. Protein concentration of the supernatant was then determined by Bradford assay after removal of the pellet. The homogenates were then labeled and visualized as described above in the inhibitor evaluation section.

Methods for Murine Pharmacokinetics Studies

All murine PK studies were carried out at NCI-Frederick. NCI-Frederick is accredited by AAALACi and follows the Public Health Service Policy on the Care and Use of Laboratory Animals. Animal care was provided in accordance with the procedures outlined in the Guide for Care and Use of Laboratory Animals (NIH publication No. 86-23, 1985). Young-adult, male nu/nu Ncr mice (average body weight of ~26 g; Animal Production Program, NCI, Frederick, MD) were used in the PK studies. Animals were maintained on hardwood chip bedding in temperature-controlled rooms (20°C) with a 12 hr light-dark cycle. Standard diet (Rat and Mouse 18% Protein Diet, PMI Nutrition International, Inc., Brentwood, MO) and water were provided ad libitum. Housing, animal care, and all experimental procedures and manipulations were carried out in an AAALACi-accredited facility in strict compliance with the National Institutes of Health guidelines for the care and use of laboratory animals and were approved by the NCI-Frederick Animal Care and Use Committee.

Pharmacokinetics Studies

Each analog was administered to mice by IV (tail vein) and IP injection, and by oral gavage (PO) at a dose of 50 mg/kg. Two mice were used for each route of administration. All analogs were dissolved in DMSO and given in a dose volume of 1 ml/kg. For each route of administration, plasma was collected from the retro-orbital sinus of one mouse after 5, 30, and 120 min and from the other mouse after 15, 60, and 90 min. Blood was collected into heparinized microfuge tubes and immediately chilled in an ice bath for 1 min. Samples were then centrifuged at 13,000 × g for 3 min in a refrigerated centrifuge (4°C), and plasma was separated, flash frozen, and stored at −70°C until assayed.

HPLC-Mass Spectrometry Assay

Samples were prepared for analysis by adding 150 μl ice-cold methanol to 50 μl plasma, followed by vigorous mixing. The mixture was then centrifuged at 13,000 × g for 12 min, the supernatant (150 μl) was removed and mixed with 450 μl 0.1% formic acid, and 580 μl was injected onto the column. Samples were analyzed with an Agilent (Agilent Technologies, Palo Alto, CA) HPLC/MS system, consisting of 1100 Series chromatographic modules interfaced with an ion trap MS module (model G2445A) controlled through a Windows NT-based ChemStation. Chromatography was conducted at ambient temperature by using a 4.6 × 250 mm I.D. Atlantis C_{18} column (Waters, Inc., Milford, MA), eluted isocratically (flow rates ranging from 0.6 to 0.75 ml/minute) with a mobile phase composed of acetonitrile-0.1% formic acid (proportions ranging from 15:85, v/v to 25:75, v/v), the precise circumstances being dependent on the optimal conditions required for each analog. The column effluent was introduced into the MS module operated under positive ion electrospray conditions in scanning mode (100–2200 *m/z*), and the appropriate mass ion for each analog was extracted during data analysis. In our hands, we found the ester analogs to hydrolyze immediately in plasma (data not shown), prompting us to monitor ions for the corresponding carboxylic acids rather than those of the parent compounds, for these molecules. Under the conditions described, retention times of the analogs varied from 8 to 13 min, and the lower limits of quantification (loq; defined as the lowest concentration that could be quantified with acceptable reproducibility [RSD < 15%]) ranged from 0.1 to 0.8 μM. Calibration curves were constructed by plotting the respective peak areas against the known analyte concentration in plasma standards. Typically, seven to eight standards covering a concentration range from the loq to 10 μM were employed. Weighted, linear least-squares regression analysis was performed to determine the slope and y intercept of the best-fit line. Analyte concentrations in unknown samples were calculated by interpolation from the regression line. Each unknown sample was assayed in duplicate, and the average of the assayed values was used for data analysis.

Pharmacokinetic Analysis

The beginning and ending times for the injection and the collection intervals were recorded to the nearest second. Plasma concentration versus time profiles were constructed by using the plasma concentration for the individual animal at each time point and the time of collection. The time of collection was calculated from the beginning of the administration to the midpoint of the sample-collection interval. Areas under the curve (AUC) were calculated by "trapezoidal rule" from time 0 to the last time point at which the analog was detected. The biological half-life was estimated by nonlinear regression analysis when the data permitted such analysis. The bioavailable fraction (%F) was calculated by dividing the AUC determined after IP or PO administration by the AUC determined after IV administration for each analog.

Supplemental Data

Supplemental Data include pharmacokinetic values along with LC-MS spectra of representative compounds and are available at http://www.chembiol.com/cgi/content/full/14/5/499/DC1/.

ACKNOWLEDGMENTS

This research was supported by grants from the National Institutes of Health (NIH), U54 RR020843, R01 EB005011, and P01 CA072006 (M.B.); the V Society for Cancer Research (J.A.J.); and the Goodwin Foundation for Cancer Research and Experimental Therapeutics (J.A.J.). This project has been funded in part with federal funds from the National Cancer Institute (NCI), NIH, under contract NO1-CO-12400. The content of this publication does not necessarily reflect the views or policies of the Department of Health and Human Services, nor does mention of trade names, commercial products, or organizations imply endorsement by the U.S. Government. This research was supported in part by the Developmental Therapeutics Program, Division of Cancer Treatment and Diagnosis, NCI, NIH.

Received: December 4, 2006
Revised: February 16, 2007
Accepted: March 13, 2007
Published: May 29, 2007

REFERENCES

1. Lecaille, F., Kaleta, J., and Bromme, D. (2002). Human and parasitic papain-like cysteine proteases: their role in physiology and pathology and recent developments in inhibitor design. Chem. Rev. *102*, 4459–4488.
2. Murata, M., Miyashita, S., Yokoo, C., Tamai, M., Hanada, K., Hatayama, K., Towatari, T., Nikawa, T., and Katunuma, N. (1991). Novel epoxysuccinyl peptides. Selective inhibitors of cathepsin B, in vitro. FEBS Lett. *280*, 307–310.
3. Towatari, T., Nikawa, T., Murata, M., Yokoo, C., Tamai, M., Hanada, K., and Katunuma, N. (1991). Novel epoxysuccinyl peptides. A selective inhibitor of cathepsin B, in vivo. FEBS Lett. *280*, 311–315.
4. Stern, I., Schaschke, N., Moroder, L., and Turk, D. (2004). Crystal structure of NS-134 in complex with bovine cathepsin B: a two-headed epoxysuccinyl inhibitor extends along the entire active-site cleft. Biochem. J. *381*, 511–517.
5. Turk, D., Podobnik, M., Popovic, T., Katunuma, N., Bode, W., Huber, R., and Turk, V. (1995). Crystal structure of cathepsin B inhibited with CA030 at 2.0-Å resolution: a basis for the design of specific epoxysuccinyl inhibitors. Biochemistry *34*, 4791–4797.
6. Bogyo, M., Verhelst, S., Bellingard-Dubouchaud, V., Toba, S., and Greenbaum, D. (2000). Selective targeting of lysosomal cysteine proteases with radiolabeled electrophilic substrate analogs. Chem. Biol. *7*, 27–38.
7. Schaschke, N., Assfalg-Machleidt, I., Lassleben, T., Sommerhoff, C.P., Moroder, L., and Machleidt, W. (2000). Epoxysuccinyl peptide-derived affinity labels for cathepsin B. FEBS Lett. *482*, 91–96.
8. Schaschke, N., Assfalg-Machleidt, I., Machleidt, W., and Moroder, L. (1998). Substrate/propeptide-derived endo-epoxysuccinyl peptides as highly potent and selective cathepsin B inhibitors. FEBS Lett. *421*, 80–82.
9. Verhelst, S.H., and Bogyo, M. (2005). Solid-phase synthesis of double-headed epoxysuccinyl activity-based probes for selective targeting of papain family cysteine proteases. Chembiochem *6*, 824–827.
10. Link, J.O., and Zipfel, S. (2006). Advances in cathepsin S inhibitor design. Curr. Opin. Drug Discov. Devel. *9*, 471–482.
11. Yasuda, Y., Kaleta, J., and Bromme, D. (2005). The role of cathepsins in osteoporosis and arthritis: rationale for the design of new therapeutics. Adv. Drug Deliv. Rev. *57*, 973–993.
12. Kim, T.S., and Tasker, A.S. (2006). Non-covalent cathepsin K inhibitors for the treatment of osteoporosis. Curr. Top. Med. Chem. *6*, 355–360.
13. Yamashita, D.S., Marquis, R.W., Xie, R., Nidamarthy, S.D., Oh, H.J., Jeong, J.U., Erhard, K.F., Ward, K.W., Roethke, T.J., Smith, B.R., et al. (2006). Structure activity relationships of 5-, 6-, and 7-methyl-substituted azepan-3-one cathepsin K inhibitors. J. Med. Chem. *49*, 1597–1612.
14. Black, W.C., and Percival, M.D. (2006). The consequences of lysosomotropism on the design of selective cathepsin K inhibitors. ChemBioChem *7*, 1525–1535.
15. Falgueyret, J.P., Black, W.C., Cromlish, W., Desmarais, S., Lamontagne, S., Mellon, C., Riendeau, D., Rodan, S., Tawa, P., Wesolowski, G., et al. (2004). An activity-based probe for the determination of cysteine cathepsin protease activities in whole cells. Anal. Biochem. *335*, 218–227.
16. Methot, N., Vaillancourt, J.P., Huang, J., Colucci, J., Han, Y., Menard, S., Zamboni, R., Toulmond, S., Nicholson, D.W., and Roy, S. (2004). A caspase active site probe reveals high fractional inhibition needed to block DNA fragmentation. J. Biol. Chem. *279*, 27905–27914.
17. Speers, A.E., and Cravatt, B.F. (2004). Profiling enzyme activities in vivo using click chemistry methods. Chem. Biol. *11*, 535–546.
18. Joyce, J.A., Baruch, A., Chehade, K., Meyer-Morse, N., Giraudo, E., Tsai, F.Y., Greenbaum, D.C., Hager, J.H., Bogyo, M., and Hanahan, D. (2004). Cathepsin cysteine proteases are effectors of invasive growth and angiogenesis during multistage tumorigenesis. Cancer Cell *5*, 443–453.
19. Satoyoshi, E. (1992). Therapeutic trials on progressive muscular dystrophy. Intern. Med. *31*, 841–846.
20. Katunuma, N., Murata, E., Kakegawa, H., Matsui, A., Tsuzuki, H., Tsuge, H., Turk, D., Turk, V., Fukushima, M., Tada, Y., and Asao, T. (1999). Structure based development of novel specific inhibitors for cathepsin L and cathepsin S in vitro and in vivo. FEBS Lett. *458*, 6–10.
21. Sumiya, S., Yoneda, T., Kitamura, K., Murata, M., Yokoo, C., Tamai, M., Yamamoto, A., Inoue, M., and Ishida, T. (1992). Molecular design of potent inhibitor specific for cathepsin B based on the tertiary structure prediction. Chem. Pharm. Bull. (Tokyo) *40*, 299–303.
22. Greenbaum, D.C., Arnold, W.D., Lu, F., Hayrapetian, L., Baruch, A., Krumrine, J., Toba, S., Chehade, K., Brèomme, D., Kuntz, I.D., and Bogyo, M. (2002). Small molecule affinity fingerprinting. A tool for enzyme family subclassification, target identification, and inhibitor design. Chem. Biol. *9*, 1085–1094.
23. Schaschke, N., Assfalg-Machleidt, I., Machleidt, W., Turk, D., and Moroder, L. (1997). E-64 analogues as inhibitors of cathepsin B. On the role of the absolute configuration of the epoxysuccinyl group. Bioorg. Med. Chem. *5*, 1789–1797.
24. Sadaghiani, A.M., Verhelst, S.H., and Bogyo, M. (2006). Solid-phase methods for the preparation of epoxysuccinate-based inhibitors of cysteine proteases. J. Comb. Chem. *8*, 802–804.
25. Greenbaum, D.C., Baruch, A., Grainger, M., Bozdech, Z., Medzihradszky, K.F., Engel, J., DeRisi, J., Holder, A.A., and Bogyo, M. (2002). A role for the protease falcipain 1 in host cell invasion by the human malaria parasite. Science *298*, 2002–2006.
26. Leung, D., Hardouin, C., Boger, D.L., and Cravatt, B.F. (2003). Discovering potent and selective reversible inhibitors of enzymes in complex proteomes. Nat. Biotechnol. *21*, 687–691.
27. Goulet, B., Baruch, A., Moon, N.S., Poirier, M., Sansregret, L.L., Erickson, A., Bogyo, M., and Nepveu, A. (2004). A cathepsin L isoform that is devoid of a signal peptide localizes to the nucleus in S phase and processes the CDP/Cux transcription factor. Mol. Cell *14*, 207–219.
28. Tamai, M., Omura, S., Kimura, M., Hanada, K., and Sugita, H. (1987). Prolongation of life span of dystrophic hamster by cysteine proteinase inhibitor, loxistation (EST). J. Pharmacobiodyn. *10*, 678–681.
29. Kominami, E., Tsukahara, T., Bando, Y., and Katunuma, N. (1987). Autodegradation of lysosomal cysteine proteinases. Biochem. Biophys. Res. Commun. *144*, 749–756.
30. Hanahan, D. (1985). Heritable formation of pancreatic β-cell tumours in transgenic mice expressing recombinant insulin/simian virus 40 oncogenes. Nature *315*, 115–122.